Light Directs Monomer Coordination in Catalyst-Free Grignard Photopolymerization.

Eliot F. Woods,[1] Alexandra J. Berl,[1] Leanna P. Kantt,[1] Michael R. Wasielewski,[1] Brandon E. Haines,[2*] and Julia A. Kalow[1*]

[1]Department of Chemistry, Northwestern University, 2145 Sheridan Rd, Evanston, IL 60208

[2]Department of Chemistry, Westmont College, 955 La Paz Rd, Santa Barbara, CA 93108.

ABSTRACT: π-Conjugated polymers can serve as active layers in flexible and lightweight electronics, and are conventionally synthesized by transition-metal-mediated polycondensation at elevated temperatures. We recently reported a photopolymerization of electron-deficient heteroaryl Grignard monomers that enables the catalyst-free synthesis of n-type π-conjugated polymers. Herein we provide an experimental and computational investigation of the mechanism of this photopolymerization. Spectroscopic studies performed in situ and after quenching suggest that the propagating species is a radical anion with halide end groups. DFT calculations for model oligomers suggest a Mg-templated $S_{RN}1$-type coupling, in which Grignard monomer coordination to the radical anion chain avoids the formation of free sp^2 radicals and enables C–C bond formation with very low barriers. We find that light plays an unusual role in the reaction, photoexciting the radical anion chain to shift electron density to the termini and thus favor productive monomer binding.

Introduction

π-Conjugated polymers (CPs) are largely synthesized via thermal transition-metal mediated cross-coupling reactions.[1] These polycondensations are ubiquitous in CP synthesis, but rely on transition-metal catalysts that can be challenging to remove.[2–5] New methods have been developed to overcome the limitations of these polycondensations through new reaction mechanisms. Highly selective C-H bond activation methods have been applied to CPs to simplify monomer preparation, reduce waste, and facilitate purification.[6–11] Recently, there have been several reports detailing new photochemical routes to CPs, which enable photopatterning and provide access to new architectures.[12–15] Photochemical methods have largely been applied to electron-rich (p-type) CPs, while methods that provide electron-poor (n-type) CPs have lagged.[16,17] For devices that use CPs, such as flexible electronics and light weight solar cells, both high performance p-type and n-type materials are required.[18] New reactions and a deeper understanding of their mechanisms are needed to improve the utility of CPs. To expand synthetic access to n-type conjugated polymers, we developed the photopolymerization of electron-poor aryl Grignard monomers using visible light (Figure 1a).[19] This polymerization has characteristics consistent with an uncontrolled chain-growth mechanism, allowing us to synthesize a fully conjugated n-type block copolymer.

Several aspects of this light-mediated polymerization merited further study. In contrast to other polycondensations of Grignard reagents, this reaction proceeds without a transition-metal catalyst, requiring only lithium chloride (LiCl)-saturated THF and light. Dark control reactions yielded oligomers (degree of polymerization, DP < 5), and higher molecular weight polymers were only produced with visible light irradiation (Figure 1b). LiCl was also found to be essential to achieve higher molecular weights and yields. While Grignards are known to form reactive "turbo Grignards" in solution with LiCl,[20,21] the improvements in reaction performance with increased LiCl were well beyond the stoichiometric quantities needed to form such complexes, suggesting a more nuanced role in the reaction (Figure 1c). Finally, the photopolymerization proved compatible with several n-type homopolymers and donor-acceptor polymers, but when applied to common electron-rich monomers, such as 3-hexylthiophene, produced only trace oligomer (Figure 1d).

Previous work has described the catalyst-free cross-coupling reaction between aryl Grignards and aryl halides as a radical-nucleophilic aromatic substitution process ($S_{RN}1$ reaction).[22,23] Unlike our polymerization, reactions that access small-molecule biaryls and meta-linked poly(arylenes) rely on high temperatures and long reaction times. Hayashi used radical clock experiments to rule out free aryl radical intermediates in this reaction; furthermore, aryl radicals generated from diazonium salts overwhelmingly underwent hydrogen atom transfer rather than C–C bond formation.[22] A computational investigation by Haines and Wiest[24] provided an explanation for the absence of detectable free aryl radical intermediates. In their revised mechanism (Scheme 1), coordination of the aryl Grignard to the aryl halide radical anion allows the resulting aryl radical intermediate to be captured by Mg^{2+} in an ion-radical cage. Collapse into a new Csp^2–Csp^2 bond occurs rapidly. All the proposed steps after rate-determining SET were found to have very low barriers (< 3 kcal/mol).

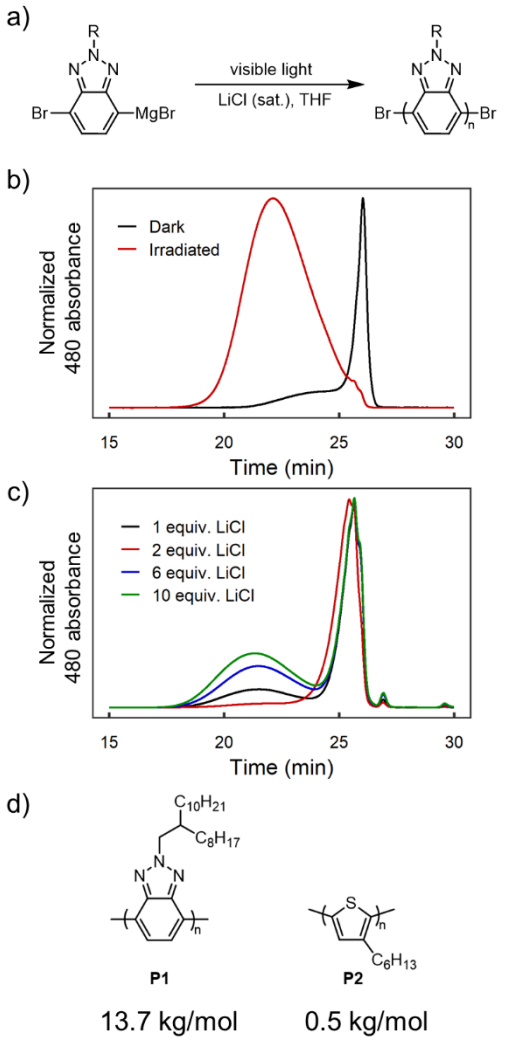

Figure 1. a) Gel permeation chromatography (GPC) traces of photopolymerization of **P1** using conditions from ref 12, with and without light. b) GPC traces showing the effect of LiCl on polymer molecular weight distribution for the photopolymerization of **P1**. c) Representative molecular weights of n-type (**P1**) and p-type (**P2**) polymers.

Herein we report an experimental and computational mechanistic study of the photocontrolled synthesis of n-type conjugated polymers, revisiting the Grignard-directed $S_{RN}1$ mechanism in the context of our polymerization. Differences between the small-molecule system and the polymer system explain key experimental observations such as the need for photoexcitation, LiCl, and the preference for electron-poor polymers. We uncover an unusual example of a photocontrolled reaction in which light redistributes electron density in the substrate to overcome unfavorable ground-state equilibria.

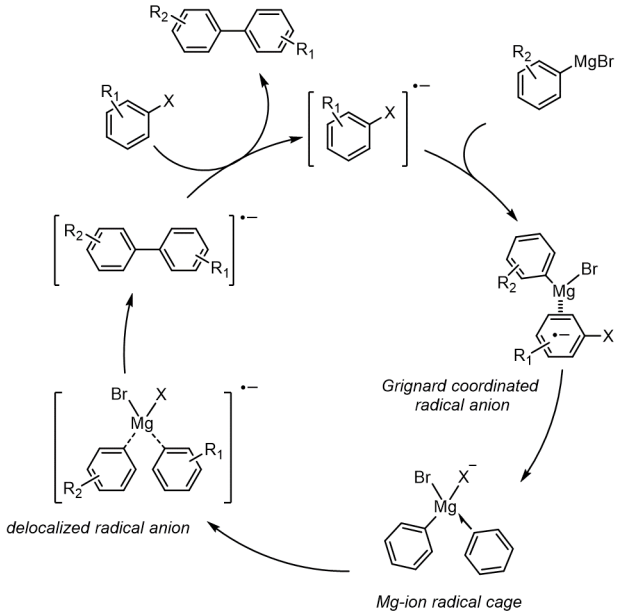

Scheme 1: Proposed mechanism of the coupling between aryl Grignard reagents and aryl halides

Results and Discussion

Propagating polymer chains are bromide-capped radical anions

We sought to experimentally determine the nature of the growing polymer chain in the reaction. Polymers isolated by precipitation into methanol MeOH from the photopolymerization of **P1** exhibit a mixture of Br/Br, Br/H, and H/H chain ends by MALDI-TOF-MS (Figure S2). However, dynamic equilibria of Grignard species in solution complicate this analysis.[25–27] To better characterize the active chain-end of growing polymers during the reaction, we designed an in-situ aldehyde chain-trapping experiment (Scheme 2).

4,7-Dibromo-2-(2-octyldodecyl)-2H-benzo[d][1,2,3]triazole was converted to a mono-Grignard reagent (**1-MgBr**) and subjected to standard photopolymerization conditions (see ref 12 for details). After four hours of irradiation, at which point polymers are still propagating, 2,6-difluorobenzaldehyde was injected into the polymerization. The reaction allowed to continue for 20 hours prior to quenching by precipitation into MeOH. Fractionation of the reaction by precipitation into acetone shows no incorporation of the fluorinated aldehyde by ^{19}F NMR in either polymer or oligomer fractions (Figure S5). Concentration of supernatant yielded the small-molecule products, which showed a new ^{19}F NMR signal distinct from 2,6-difluorobenzaldehyde. This new product was isolated and determined to be the product of Grignard monomer addition to the aldehyde (**3**) (see SI for details). These results suggest that the propagating polymers are capped by bromine, not magnesium. The Br/Br chain-ends likely come about through an initial oxidative dimerization of Grignard monomers mediated by adventitious oxygen, as has been previously reported in the literature.[28–30] We hypothesize that protonated chain ends, observed by MALDI-TOF-MS, result from Grignard metathesis between monomer and polymer chains, a possible termination pathway for the polymerization.

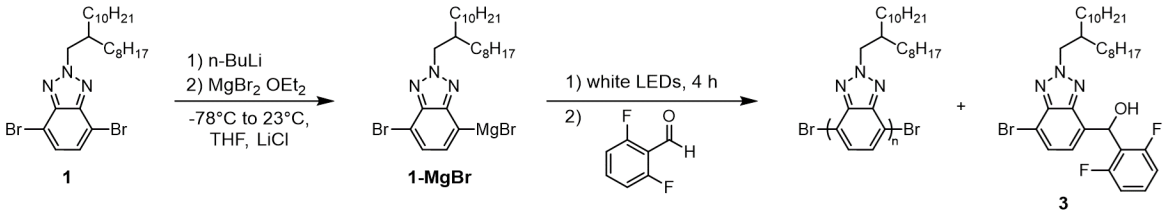

Scheme 2: Aldehyde chain-end capping experiment.

Having identified the chain end, we then went on to characterize the electronic state of the growing polymer. The mechanistic study by Haines and Wiest proposed that the reaction is propagated by aryl halide radical anions.[24] Given the evidence of brominated chain-ends, if the growing polymers were found to be radical anions, it could suggest that the polymerization operates under a similar mechanism. Indeed, continuous wave electron paramagnetic resonance (CW-EPR) of the polymerization shows radical character (Figure 2). CW-EPR of **1-MgBr** before irradiation shows no signal, suggesting that radical character seen in the reaction is associated with the polymer. Isolated **P1** also shows no radical character by CW-EPR, but **P1** treated with of sodium napthalenide (1 equivalent per polymer chain) show a similar EPR signal, further suggesting that radical character must be associated with the polymer chains. Taken together, the chain-end capping and CW-EPR experiments suggest that the growing polymers are bromine capped radical anions.

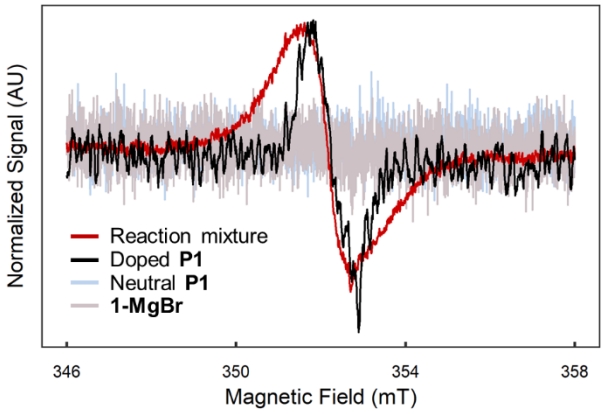

Figure 2. Continuous wave electron paramagnetic resonance spectra of neutral **P1**, n-type doped **P1**, **1-MgBr**, and polymerization reaction mixture of **P1** (see SI for details).

LiCl prevents monomer coordination to heteroatoms along the polymer chain

With a better understanding of the identity of the growing polymer chain, we began our computational investigation using density functional theory (DFT, CAM-B3LYP/6-311G(d) CPCM (THF)) calculations[31], using the dibrominated benzotriazole dimer radical anion as a model. Three major coordination modes of the monomer to the radical anion were located (Figure 3a). The two lowest-energy coordination modes are at the chain-end (**4**) and internal nitrogen (**5**) positions of the benzotriazole ring. Coordination to the π-system of the aromatic ring (**6**), which is required for abstracting the chain-end bromine, is 9.3 and 7.0 kcal/mol higher in free energy than the nitrogen coordination structures **4** and **5**, respectively. These data suggest that nitrogen coordination could be a significant unproductive trap for the Grignard monomer.

We hypothesized that LiCl could coordinate the nitro-gen atoms and free up the Grignard monomer for produc-tive reactions. Indeed, we found that a THF-solvated lithi-um cation can displace the Grignard monomer from chain end nitrogen sites in a model reaction ($\Delta G° = -11.1$ kcal/mol, Figure 3b). These calculations suggest that su-perstoichiometric quantities of LiCl improve the reaction by pushing this equilibrium further to the right, saturating the nitrogen "trap" sites on the polymer to disfavor un-productive monomer binding.

Energy landscape of dimer carbon-bromine bond scission and C–C bond formation

As the forward reaction requires the Grignard at the chain end to abstract bromide, we investigated the energy landscape as the monomer approaches the C–Br bond in the radical anion dimer (Figure 4a). A transition state, **TS-1**, was identified along the reaction pathway between monomer bound to the meta position in **6** and an ipso-coordinated structure (**8**). Intrinsic reaction coordinate analysis of **TS-1** connects to a metastable ortho-coordinated structure (**7**) that falls to **6** upon optimization. This suggests the process of monomer migration to the ipso carbon can proceed carbon-by-carbon along the ring. Geometric analysis of **TS-1** indicates that the migration is coupled with concomitant bending of the C–Br bond (164° out of aryl plane). A similar bending was observed in the small-molecule study and can be attributed to the intra-molecular electron transfer of the unpaired electron from the π system to the C–Br σ* orbital.[24,32–38] Overall, the migration of the Grignard to the ipso carbon requires a barrier of 9.4 kcal/mol. Alternatively, as the energies for **6** and **8** coordination are close in energy ($\Delta G° = 0.7$ kcal/mol) it is also possible that monomer could directly coordinate to the ipso carbon from solution.

From **8**, there is a small barrier of 4.2 kcal/mol to break the carbon bromine bond (**TS-2**) and reach a Mg-ion-radical cage complex (**9**). A spin density map of **9** (Figure 4a inset) shows that the radical is localized onto the ipso carbon of the dimer. As shown in Figure 4b, there is a 0.7 kcal/mol barrier for the aryl ring of the monomer of **9** to rotate (**TS-3**), allowing delocalization of the unpaired electron across the two aryl systems through Mg (**10**, spin density Figure 4b inset). The delocalized radical structure then passes through another low barrier of 3.1 kcal/mol (**TS-4**) to form the new C–C bond. The small barriers of all steps related to C–C bond formation suggest that once formed, **9** is rapidly converted to product, explaining why rapid termination due to free sp^2 radicals is not observed.

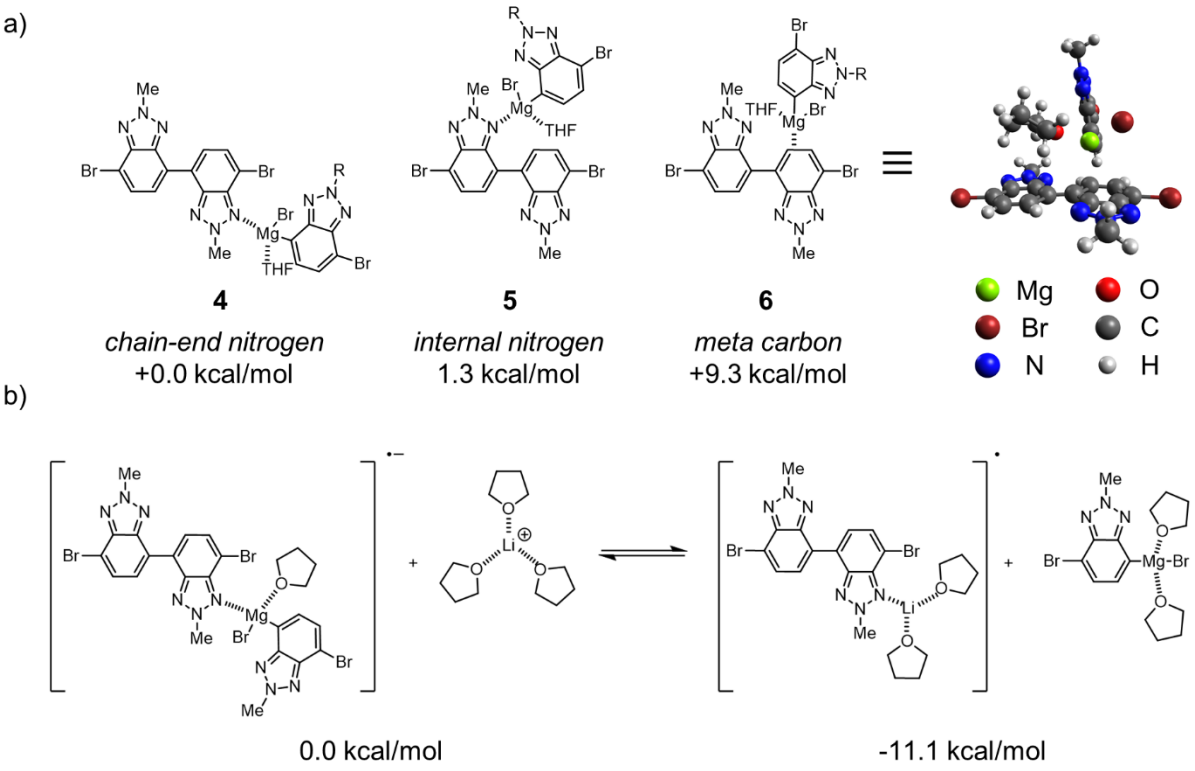

Figure 3. a) Grignard monomer coordination structures of benzotriazole dimer radical anion (computed structure for meta carbon coordination included). Gibbs free energies are relative to chain-end nitrogen coordination. b) Computed relative Gibbs free energy for the equilibrium between monomer versus lithium cation coordination at chain-end nitrogen sites on the benzotriazole radical anion dimer.

Light shifts electron density towards the chain-end in larger oligomers and polymers

The energetics of the steps shown in Figures 4 for the dimer suggest that the processes of breaking the chain-end C–Br bond and forming the new C–C bond are thermodynamically favorable, with low kinetic barriers. From this energy landscape, light does not appear to be necessary for these steps. Indeed, our control experiments suggest that the first several monomer additions (up to DP 4) can occur without light.[19] We therefore turned our attention to chains of longer length to understand the role of light in the polymerization. We hypothesized that internal positions of the growing polymer chain could compete with the chain end for monomer coordination. These interactions will become increasingly important as the polymer chain grows, and the number of potential unproductive binding sites for the monomer increases.

Based on studies of **P1** by Seferos,[39] we used the benzotriazole hexamer to model a polymer that has reached the effective conjugation length. Indeed, we find that in the hexamer, monomer binding to the chain end is no longer favorable in the ground state (Figure 5). Binding to internal monomer units is >17 kcal/mol more favorable than the chain-end benzotriazole (Figure 5a). This large difference in stability can be rationalized by visualization of the HOMO of the hexamer radical anion (Figure 5b), which shows significant localization of electron density on the inner monomer units. This shift of electron density away from the chain ends has been previously observed in studies of n-doped CPs.[40–42] This phenomenon is attributed to excess charge moving to the site of longest conjugation to minimize the energy of the polymer, resulting in a relative depletion at the chain ends.

Therefore, we performed time dependent density functional theory (TD-DFT) calculations to visualize the electronic excitations of the hexamer radical anion to its lowest excited state (the ^{1}D doublet state). Density difference plots comparing the electron density in the ground and first excited state (^{0}D and ^{1}D respectively) show a clear shift in electron density away from the internal monomer units and towards the chain ends. Moreover, excited-state optimizations of the Grignard monomer bound to the hexamer radical anion converge to a structure with the monomer bound to the ortho-position of the chain end, suggesting that the shift in electron density translates to changes in monomer coordination (Figure S11).

Thus, the role of light in the photopolymerization can be understood: light does not directly promote bond-breaking or bond formation, but instead favors productive monomer coordination. This proposal is consistent with experimental observations of light dependence. In dark controls, low-molecular-weight oligomers are formed at room temperature, in agreement with the low barriers observed in the dimer energy landscape. Formation of higher-molecular-weight polymers requires light (Figure 1b).[19] Visualization of HOMOs of the dimer, tetramer, and hexamer (Figure S10) show a trend of increasing localization of electron density within the center for the chain as the length of conjugation increases. Excited-state geometry optimizations of the ^{1}D state for benzotriazole dimer and tetramer radical anions bound to monomer also show ortho-coordinated structures, suggesting that light could have a beneficial effect on the reaction even before polymers reach their effective conjugation length.

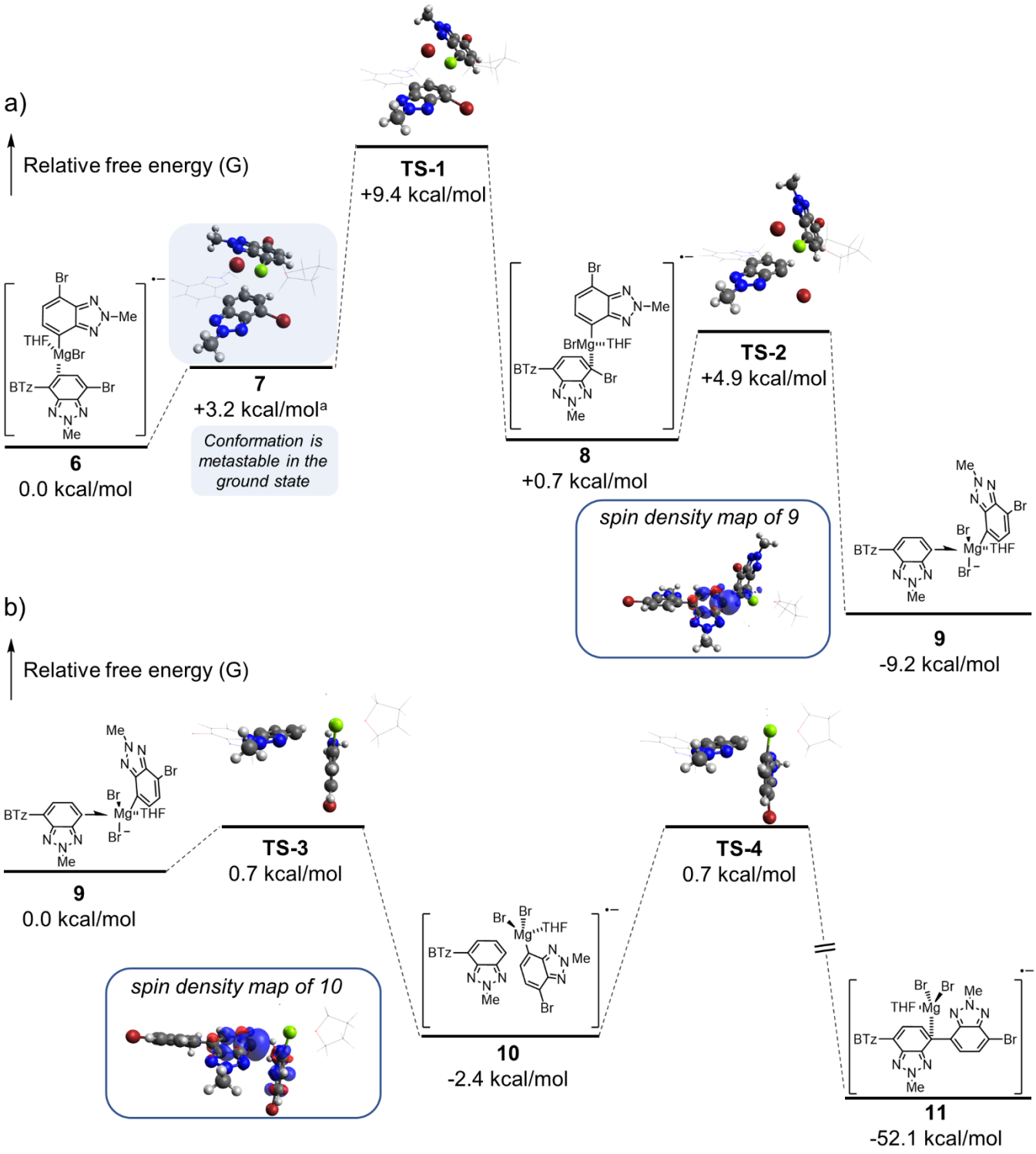

Figure 4. Benzotriazole dimer radical anion free energy surface for C-Br bond breaking (a) and C-C bond formation (b) Drawn structures have the second monomer ring truncated with "BTz" (see SI for full structures). Computational structures have second monomer unit, bromine atoms, and THF represented in wireframe for clarity. [a] The energy of this structure was estimated via constrained geometry optimization of the Mg-ipso carbon distance ob-tained from the IRC calculation of **TS-1**.

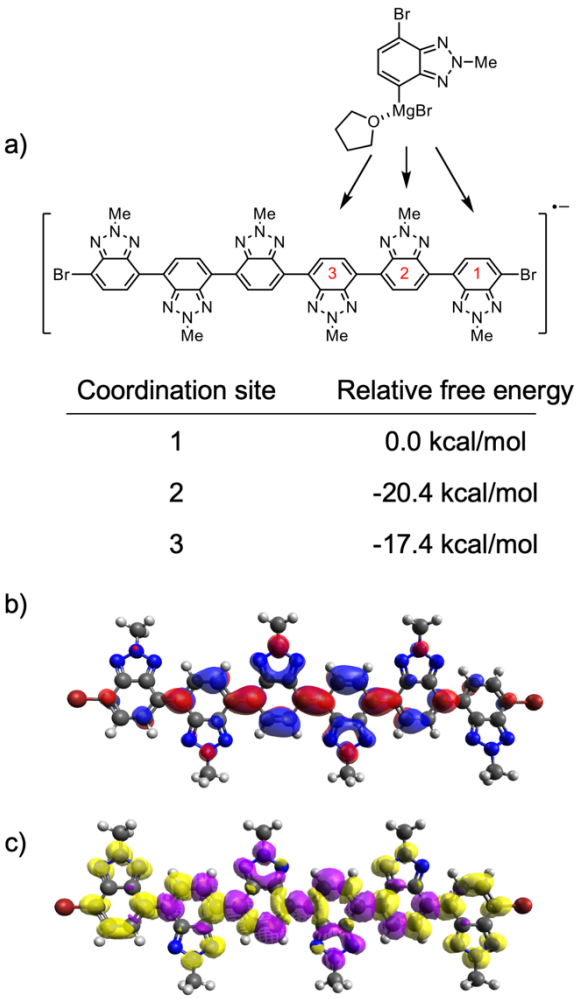

Figure 5. a) Relative Gibbs free energy of carbon-centered monomer coordination along the **P1** hexamer radical anion backbone. b) HOMO of hexamer radical anion. c) Density difference plot of the first excited state (D_1) of the hexamer radical anion compared to the ground state. Yellow indicates a relative increase (D_1 vs D_0) of electron density, and violet indicates a relative decrease.

Based on our computational and experimental results, we propose the following mechanism for propagation (Scheme 3). In the first step, the Grignard monomer samples coordination sites along the ground-state radical anion polymer chain (Scheme 3, I). Photoexcitation of the polymer chain shifts electron density away from the inner monomer units towards the chain-end, directing monomer coordination to the reaction site (Scheme 3, II). Once at the chain end, there are only small kinetic barriers for the Grignard monomer to direct the abstraction of the chain-end bromine (Scheme 3, III). The resulting Mg-radical ion cage complex then quickly collapses into a delocalized biaryl radical ion (Scheme 3, IV) that then forms the C–C bond while expelling $MgBr_2$ (Scheme 3, V). Recent computational studies suggest that there are likely many structures of the Grignard monomer in solution, which are near-degenerate in energy, and may enter this reaction via an amalgamation of similar mechanisms.[43] Regardless of the many nuances of Grignard speciation in the experimental system, we believe that the mechanism in Scheme 3 provides a general framework for understanding the reaction.

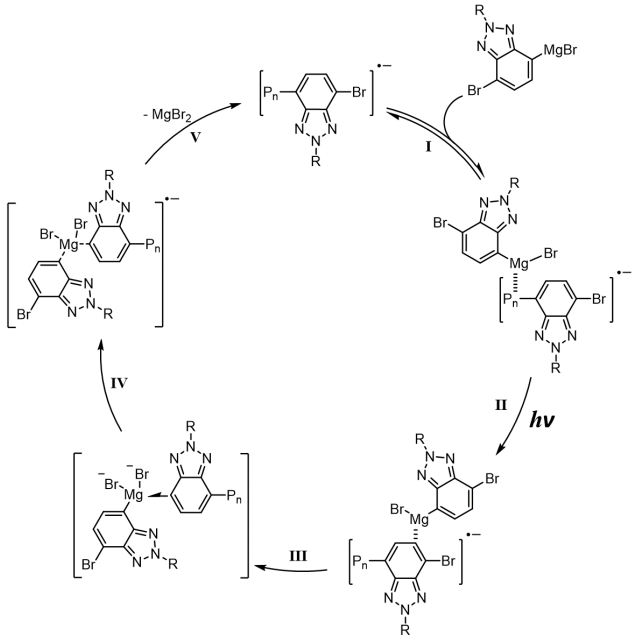

Scheme 3: Proposed mechanism for propagation in the photopolymerization of 1-MgBr.

Key features of the **1-MgBr** system are present in the other successful monomer systems reported previously.[19] The homopolymer poly(2,3-bis(2-ethylhexyl)thieno[3,4-b]pyrazine) has an electron-poor π-system and heteroaromatic sites that could compete for Grignard coordination. Similarly, benzothiadiazole and diketopyrrolopyrrole based donor-acceptor monomers that were compatible with the polymerization also contain these key features. As all polymers that could be produced via the polymerization share **P1**'s properties of heteroatoms and electron-deficient π-systems, it is likely that this mechanism is a relevant framework for understanding the catalyst-free Grignard photopolymerization.

Free-radical reactivity terminates electron rich polymers

With this mechanistic framework for the successful **P1** system, we can now begin to investigate the poor reactivity of electron-rich monomers in the photopolymerization. Polythiophene is a ubiquitous p-type polymer in the literature, often synthesized by Pd- or Ni-catalyzed polycondensation, but under our standard reaction conditions, **2-MgBr** (Figure 6a) produce <5% yield of oligomers. To understand why this reaction fails, we performed calculations for monomer coordination to the thiophene dimer radical anion, **12** (Figure 6a; the hexyl chain is truncated to CH_3), which would be produced by oxidative dimerization of 2-MgBr. The radical anion **12** shows C3 coordination analogous to **6** (Figure S9), in addition to a sulfur-coordinated structure 13 (Figure 6b). The sulfur coordinated **13** is 2.4 kcal/mol more stable than the lowest energy carbon coordination meaning this coordination mode suggesting that **13** will be the preferred coordination in solution. While the carbon-coordinated structures do not exhibit significant lengthening or bending of the C–Br bond, the sulfur-coordinated conformer exhibits C–Br bond elongation by 0.75 Å and significant spin density localization onto the carbon atom (Figure 6c, see Figure S9 for spin density maps of carbon-coordinated structures). The extent of bond breaking in this structure suggests that the electron-rich bithiophene radical anion could be undergoing bond heterolysis, analogous to a typical $S_{RN}1$ reaction. If this is the case, the resulting "free" heteroaryl radical would

likely undergo rapid hydrogen-atom abstraction from the weak C–H bonds of the THF solvent.

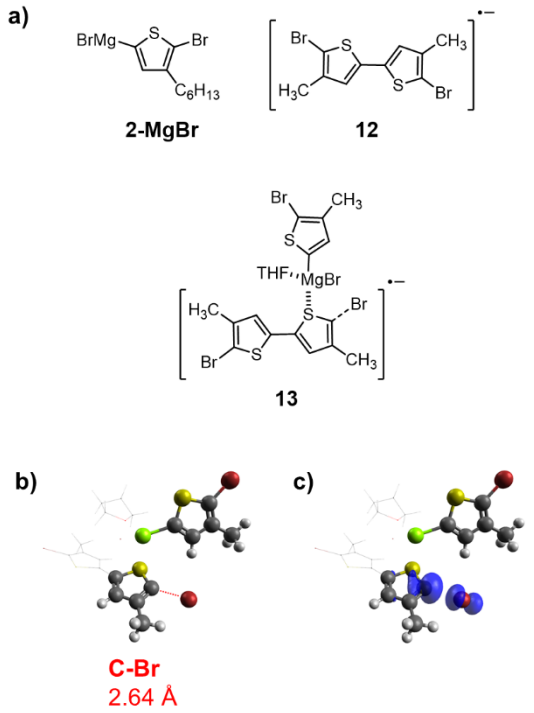

Figure 6. a) Coordination modes for monomer 2-MgBr to the bithiophene radical anion **12** and corresponding C–Br bond lengths. b) Coordination at S results in 0.75 Å elongation of the C–Br bond. c) Spin density map (isovalue 0.005) for the sulfur-coordinated conformer **13**.

To test this hypothesis and the physical significance of the sulfur-coordinated structure, the photopolymerization of **2-MgBr** was conducted in THF-d_8 and THF (Figure 7). Isolated oligomers from each reaction (n=3) show a clear +1 m/z shift by MALDI-TOF-MS that is consistent with deuterium incorporation. ^{2}D incorporation is additionally observed by ^{2}H NMR for the THF-d_8 reaction, but not in THF (Figure 7). In contrast, when **1-MgBr** is polymerized in THF-d_8, no deuterium incorporation is seen by ^{2}H NMR (Figure S6) or MALDI-TOF-MS (Figure S7).

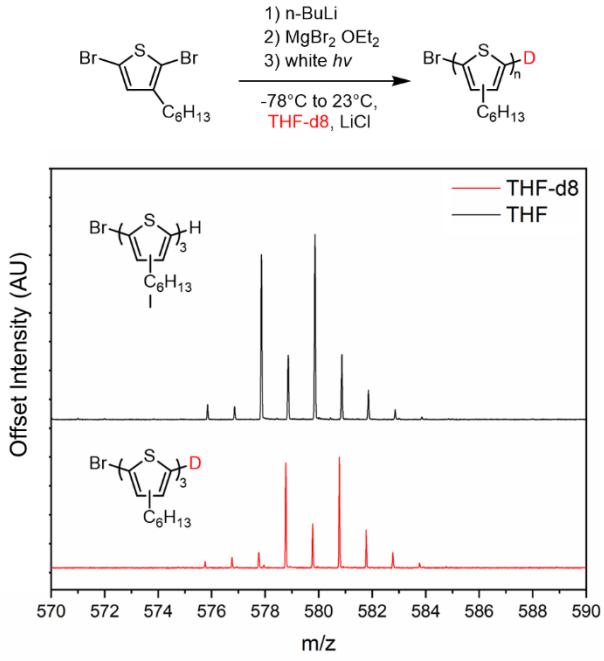

Figure 7. Photopolymerization of 2,5-dibromo-3-hexylthiophene in THF-d_8 (top) and MALDI-TOF-MS comparison of isolated trimer from THF-d_8 polymerization and THF polymerization.

Our previous work showed that other polymers with sulfur heteroatoms, poly(2,3-bis(2-ethylhexyl)thieno[3,4-b]pyrazine) and poly(2-(2-octyldodecyl)-4,7-di(thiophen-2-yl)-2H-benzo[d][1,2,3]triazole), were compatible with the photopolymerization, suggesting that this termination cannot be attributed to sulfur coordination alone.[19] Like thiophene, an electronically neutral hydrocarbon monomer 2,7-dibromo-9,9-dioctyl-9H-fluorene produced only trace oligomer.[19] Computational modeling of monomer coordination to a fluorene dimer radical anion showed bromine abstraction and dissociation of the Grignard reagent, suggesting that C–Br bond scission to form free radicals is primarily related to monomer electronics (Figure S12). Taken together, the computed dimer radical anion structures and THF-d_8 reactions suggest that electron-neutral and -rich monomers fail under the photopolymerization conditions due to $S_{RN}1$ pathways that form rapidly terminated sp^2 radicals.

Conclusion

In summary, we have experimentally and computationally explored the photopolymerization of aryl Grignard monomers. These studies reveal a Mg-templated $S_{RN}1$ reaction analogous to the thermal small-molecule version, but explains why those conditions fail for polymerization. Our calculations suggest that for electron-deficient heteroaromatic monomers, once the Grignard monomer coordinates to the polymer chain end, the barriers to bromide abstraction and C–C bond formation are exceptionally low. The rapid rate of these steps and delocalization of the radical intermediate minimizes side reactions that would be expected for free sp^2 radicals in a traditional $S_{RN}1$ process. The extended π-system of the growing polymer chain and abundance of coordinating heteroatoms necessitate key modifications to the thermal small-molecule reaction; namely, irradiation by visible light and excess LiCl. In combination, LiCl and light funnel Grignard monomers to the reactive chain-end sites. High concentrations of LiCl block the heteroatom sites of the

polymer chain, promoting Grignard monomer coordination along the pi-system of the polymer backbone. As the chain grows, unproductive Grignard monomer binding to inner sites of the polymer backbone dominate, and photoexcitation is required to shift electron density to the chain ends and favor productive binding events. Furthermore, this mechanistic study provides insight into the incompatibility of electron-rich and -neutral monomers with the photopolymerization. These radical anions undergo facile C–Br heterolysis, resulting in unstabilized sp^2 radicals that undergo termination by H-atom abstraction.

This light-promoted, Mg-templated $S_{RN}1$ reaction may be contrasted to the state-of-the-art in controlled CP synthesis, catalyst-transfer polycondensation (CTP).[16,44] Like CTP, the photopolymerization mechanism requires coordination of an organometallic species to the π-system of the growing polymer chain. Unlike CTP, however, the coordination does not need to be maintained throughout propagation to enforce a chain-growth mechanism; selective photoexcitation and residence of the radical anion along the growing chain favor chain growth over monomer-monomer coupling. However, uncontrolled initiation by adventitious oxygen and termination by Grignard metathesis remain drawbacks of our photocontrolled CP synthesis.

This work illustrates a highly unusual role for light in modulating the substrate electronics to promote productive binding, and an alternative to more common triplet sensitization and single-electron-transfer mechanisms. As CTP also relies on coordination of organometallic species to the polymer chain, we anticipate that this insight will inspire the development of new photo-mediated variants. Future work will focus on using these mechanistic insights to identify new monomer designs that are compatible with the reaction and produce high-performance CPs, and studying the mechanisms of initiation and termination to exert better control over the polymerization.

ASSOCIATED CONTENT

Supporting Information.

Synthetic procedures; details of the computational methods; characterization data for new compounds; visualized HOMO and LUMOs of relevant structures; XYZ coordinates of calculated structures. This material is available free of charge via the Internet at http://pubs.acs.org.

AUTHOR INFORMATION

Corresponding Authors

* Julia A. Kalow – Department of Chemistry, Northwestern University, Evanston Illinois 60208

* Brandon E. Haines – Department of Chemistry, Westmont College, Santa Barbara, CA 93108.

Funding Sources

This work was supported by funding from the Air Force Of-fice of Scientific Research Young Investigator Program (FA9550-18-1-0159), a 3M Non-Tenured Faculty Award, and the National Science Foundation Graduate Research Fellowship Program (A.J.B., DGE-1842165). This work made use of NMR and MS instrumentation at the Integrated Molecular Structure Education and Research Center (IMSERC) at Northwestern, which has received support from the NSF (NSF CHE-9871268); Soft and Hybrid Nanotechnology Experimental (SHyNE) Resource (NSF ECCS-1542205); the State of Illinois; and the International Institute for Nanotechnology.

ACKNOWLEDGMENT

This research was supported in part through the computational resources and staff contributions provided for the Quest high performance computing facility at Northwestern University which is jointly supported by the Office of the Provost, the Office for Research, and Northwestern University Information Technology.

REFERENCES

(1) Xu, S.; Kim, E. H.; Wei, A.; Negishi, E. I. Pd- and Ni-Catalyzed Cross-Coupling Reactions in the Synthesis of Organic Electronic Materials. Science and Technology of Advanced Materials. Taylor & Francis 2014.

(2) Usluer, Ö.; Abbas, M.; Wantz, G.; Vignau, L.; Hirsch, L.; Grana, E.; Brochon, C.; Cloutet, E.; Hadziioannou, G. Metal Residues in Semiconducting Polymers: Impact on the Performance of Organic Electronic Devices. ACS Macro Lett. 2014, 3, 1134–1138.

(3) Bannock, J. H.; Treat, N. D.; Chabinyc, M.; Stingelin, N.; Heeney, M.; de Mello, J. C. The Influence of Polymer Purification on the Efficiency of Poly(3-Hexylthiophene):Fullerene Organic Solar Cells. Sci. Rep. 2016, 6, 23651.

(4) Krebs, F. C.; Nyberg, R. B.; Jørgensen, M. Influence of Residual Catalyst on the Properties of Conjugated Polyphenylenevinylene Materials: Palladium Nanoparticles and Poor Electrical Performance. Chem. Mater. 2004, 16, 1313–1318.

(5) Kuwabara, J.; Yasuda, T.; Takase, N.; Kanbara, T. Effects of the Terminal Structure, Purity, and Molecular Weight of an Amorphous Conjugated Polymer on Its Photovoltaic Characteristics. ACS Appl. Mater. Interfaces 2016, 8, 1752–1758.

(6) Dudnik, A. S.; Aldrich, T. J.; Eastham, N. D.; Chang, R. P. H.; Facchetti, A.; Marks, T. J. Tin-Free Direct C–H Arylation Polymerization for High Photovoltaic Efficiency Conjugated Copolymers. J. Am. Chem. Soc. 2016, 138, 15699–15709.

(7) Kuwabara, J.; Kanbara, T. Facile Synthesis of π-Conjugated Polymers via Direct Arylation Polycondensation. Bull. Chem. Soc. Jpn. 2018, 92, 152–161.

(8) Pankow, R. M.; Thompson, B. C. Approaches for Improving the Sustainability of Conjugated Polymer Synthesis Using Direct Arylation Polymerization (DArP). Polym. Chem. 2020, 11, 630–640.

(9) Kang, L. J.; Xing, L.; Luscombe, C. K. Exploration and Development of Gold- and Silver-Catalyzed Cross Dehydrogenative Coupling toward Donor–Acceptor π-Conjugated Polymer Synthesis. Polym. Chem. 2019, 10, 486–493.

(10) Huang, Y.; Luscombe, C. K. Towards Green Synthesis and Processing of Organic Solar Cells. Chem. Rec. 2019, 19, 1039–1049.

(11) King, E. R.; Tropp, J.; Eedugurala, N.; Gonce, L. E.; Stanciu, S.; Azoulay, J. D. Gold-Catalyzed C–H Functionalization Polycondensation for the Synthesis of Aromatic Polymers. Angew. Chemie Int. Ed. 2020, 59, 21971–21975.

(12) Liu, X.; Sharapov, V.; Zhang, Z.; Wiser, F.; Awais, M. A.; Yu, L. Photoinduced Cationic Polycondensation in Solid State towards Ultralow Band Gap Conjugated Polymers. J. Mater. Chem. C 2020, 8, 7026–7033.

(13) Koyuncu, S.; Hu, P.; Li, Z.; Liu, R.; Bilgili, H.; Yagci, Y. Fluorene-Carbazole-Based Porous Polymers by Photoinduced Electron Transfer Reactions. Macromolecules 2020, 53, 1645–1651.

(14) Celiker, T.; İsci, R.; Kaya, K.; Ozturk, T.; Yagci, Y. Photoinduced Step-growth Polymerization of Thieno[3,4-b] Thiophene Derivatives. The Substitution Effect on the Reactivity and Electrochemical Properties. J. Polym. Sci. 2020, pol.20200398.

(15) Woods, E. F.; Berl, A. J.; Kalow, J. A. Advances in the Synthesis of π-Conjugated Polymers by Photopolymerization. ChemPhotoChem 2021, 5, 4–11.

(16) Leone, A. K.; McNeil, A. J. Matchmaking in Catalyst-Transfer Polycondensation: Optimizing Catalysts Based on Mechanistic Insight. Acc. Chem. Res. 2016, 49, 2822–2831.

(17) Leone, A. K.; Mueller, E. A.; McNeil, A. J. The History of Palladium-Catalyzed Cross-Couplings Should Inspire the Future of Catalyst-Transfer Polymerization. J. Am. Chem. Soc. 2018, 140, 15126–15139.

(18) Jia, H.; Lei, T. Emerging Research Directions for N-Type Conjugated Polymers. J. Mater. Chem. C 2019, 7, 12809–12821.

(19) Woods, E. F.; Berl, A. J.; Kalow, J. A. Photocontrolled Synthesis of N-Type Conjugated Polymers. Angew. Chemie Int. Ed. 2020.

(20) Li-Yuan Bao, R.; Zhao, R.; Shi, L. Progress and Developments in the Turbo Grignard Reagent I-PrMgCl·LiCl: A Ten-Year Journey. Chem. Commun. 2015, 51, 6884–6900.

(21) Ziegler, D. S.; Wei, B.; Knochel, P. Improving the Halogen–Magnesium Exchange by Using New Turbo-Grignard Reagents. Chem. – A Eur. J. 2019, 25, 2695–2703.

(22) Uchiyama, N.; Shirakawa, E.; Hayashi, T. Single Electron Transfer-Induced Grignard Cross-Coupling Involving Ion Radicals as Exclusive Intermediates. Chem. Commun. 2013, 49, 364–366.

(23) Murarka, S.; Studer, A. Radical/Anionic SRN1-Type Polymerization for Preparation of Oligoarenes. Angew. Chemie Int. Ed. 2012, 51, 12362–12366.

(24) Haines, B. E.; Wiest, O. SET-Induced Biaryl Cross-Coupling: An SRN1 Reaction. J. Org. Chem. 2014, 79, 2771–2774.

(25) Ashby, E. C.; Nackashi, J.; Parris, G. E. Composition of Grignard Compounds. X. NMR, Ir, and Molecular Association Studies of Some Methylmagnesium Alkoxides in Diethyl Ether, Tetrahydrofuran, and Benzene. J. Am. Chem. Soc. 1975, 97, 3162–3171.

(26) Seyferth, D. The Grignard Reagents. Organometallics 2009, 28, 1598–1605.

(27) Peltzer, R. M.; Eisenstein, O.; Nova, A.; Cascella, M. How Solvent Dynamics Controls the Schlenk Equilibrium of Grignard Reagents: A Computational Study of CH3MgCl in Tetrahydrofuran. J. Phys. Chem. B 2017, 121, 4226–4237.

(28) Krasovskiy, A.; Tishkov, A.; del Amo, V.; Mayr, H.; Knochel, P. Transition-Metal-Free Homocoupling of Organomagnesium Compounds. Angew. Chemie Int. Ed. 2006, 45, 5010–5014.

(29) Maji, M. S.; Pfeifer, T.; Studer, A. Oxidative Homocoupling of Aryl, Alkenyl, and Alkynyl Grignard Reagents with TEMPO and Dioxygen. Angew. Chemie Int. Ed. 2008, 47, 9547–9550.

(30) Murarka, S.; Möbus, J.; Erker, G.; Mück-Lichtenfeld, C.; Studer, A. TEMPO-Mediated Homocoupling of Aryl Grignard Reagents: Mechanistic Studies. Org. Biomol. Chem. 2015, 13, 2762–2767.

(31) Full geometry optimizations of stationary points were calculated at the CAM-B3LYP/6-311G(d)/CPCM(THF) level of theory. Energies reported for stationary points are Gibbs free energies calculated at 298 K and 1.0 M standard state. See SI for full details

(32) Pierini, A. B.; Duca, J. S. Theoretical Study on Haloaromatic Radical Anions and Their Intramolecular Electron Transfer Reactions. J. Chem. Soc. Perkin Trans. 2 1995, No. 9, 1821–1828.

(33) B. Pierini, A.; S. Duca, J.; Jr., Domingo M. A. Vera, J. S. D.; M. A. Vera, D. A Theoretical Approach to Understanding the Fragmentation Reaction of Halonitrobenzene Radical Anions†. J. Chem. Soc. Perkin Trans. 2 1999, No. 5, 1003–1010.

(34) Laage, D.; Burghardt, I.; Sommerfeld, T.; Hynes, J. T. On the Dissociation of Aromatic Radical Anions in Solution. 1. Formulation and Application to p-Cyanochlorobenzene Radical Anion. J. Phys. Chem. A 2003, 107, 11271–11291.

(35) Burghardt, I.; Laage, D.; Hynes, J. T. On the Dissociation of Aromatic Radical Anions in Solution. 2. Reaction Path and Rate Constant Analysis. J. Phys. Chem. A 2003, 107, 11292–11306.

(36) Pierini, A. B.; Vera, D. M. A. Ab Initio Evaluation of Intramolecular Electron Transfer Reactions in Halobenzenes and Stabilized Derivatives. J. Org. Chem. 2003, 68, 9191–9199.

(37) Takeda, N.; Poliakov, P. V; Cook, A. R.; Miller, J. R. Faster Dissociation: Measured Rates and Computed Effects on Barriers in Aryl Halide Radical Anions. J. Am. Chem. Soc. 2004, 126, 4301–4309.

(38) Costentin, C.; Robert, M.; Savéant, J.-M. Fragmentation of Aryl Halide π Anion Radicals. Bending of the Cleaving Bond and Activation vs Driving Force Relationships. J. Am. Chem. Soc. 2004, 126, 16051–16057.

(39) McCormick, T. M.; Bridges, C. R.; Carrera, E. I.; DiCarmine, P. M.; Gibson, G. L.; Hollinger, J.; Kozycz, L. M.; Seferos, D. S. Conjugated Polymers: Evaluating DFT Methods for More Accurate Orbital Energy Modeling. Macromolecules 2013, 46, 3879–3886.

(40) Wang, S.; Sun, H.; Ail, U.; Vagin, M.; Persson, P. O. Å.; Andreasen, J. W.; Thiel, W.; Berggren, M.; Crispin, X.; Fazzi, D.; Fabiano, S. Thermoelectric Properties of Solution-Processed n-Doped Ladder-Type Conducting Polymers. Adv. Mater. 2016, 28, 10764–10771.

(41) Fazzi, D.; Fabiano, S.; Ruoko, T.-P.; Meerholz, K.; Negri, F. Polarons in π-Conjugated Ladder-Type Polymers: A Broken Symmetry Density Functional Description. J. Mater. Chem. C 2019, 7, 12876–12885.

(42) Debnath, S.; Boyle, C. J.; Zhou, D.; Wong, B. M.; Kittilstved, K. R.; Venkataraman, D. Persistent Radical Anion Polymers Based on Naphthalenediimide and a Vinylene Spacer. RSC Adv. 2018, 8, 14760–14764.

(43) Peltzer, R. M.; Gauss, J.; Eisenstein, O.; Cascella, M. The Grignard Reaction – Unraveling a Chemical Puzzle. J. Am. Chem. Soc. 2020, 142, 2984–2994.

(44) Bryan, Z. J.; Mcneil, A. J. Conjugated Polymer Synthesis via Catalyst-Transfer Polycondensation (CTP): Mechanism, Scope, and Applications. Macromolecules 2013.